Research report

Project number PN-III-P4-ID-PCE2020-0332

Title: “MicroLIBS sensors for robotic planetary and astrobiological exploration missions”/ “Senzori MicroLIBS pentru misiuni robotizate de explorare planetară și astrobiologice” - ROBIM

SCIENTIFIC REPORT - December 2022

Project director: Prof. univ. dr. habil. S. Gurlui

Webpage, project: http://spectroscopy.phys.uaic.ro/robim.html

SCIENTIFIC REPORT - December 2022

1. Introduction

The activities carried out under WP2 and WP3 have been fully (100%) completed. The aim of the research was to study effects induced by dual-pulse lasers system in interaction with matter compared to single pulsed laser system in interaction with matter and to re-create MARS environmental conditions. The study was designed in such a way that all the proposed objectives could be achieved through the conducted experiments. By conducting an experiment with a high-power pulsed laser applied to an oyster shell target, it was proven that this target offers all the necessary elements for the subject addressed. Through the heating process above the plasma threshold, the deacetylation of the chitin component was obtained with the release of acetylene and the decomposition of calcium carbonate with the release of carbon dioxide [1]. Thus, the environmental conditions specific to Mars were obtained during the experiment, and the experiment was then resumed after the set-up of the system with dual-pulsed lasers, studying the different morphological structure effects obtained in this case. The chemical effects were similar as in the case of a single pulsed laser.

References 1.

[1] Georgiana Cocean, Alexandru Cocean, Cristina Postolachi, Silvia Garofalide, Georgiana Bulai, Bogdanel Silvestru Munteanu, Nicanor Cimpoesu, Iuliana Cocean and Silviu Gurlui, High-Power Laser Deposition of Chitosan Polymers: Medical and Environmental Applications. Polymers 2022, 14, 1537. https:// doi.org/10.3390/polym14081537

2. Materials and Method of Work

The study is aimed to identify changes in the morphological and chemical structure of the materials consisting of polymers during ablation and deposition in vacuum conditions when for irradiation, a dual-pulsed lasers system (DPL) is used.

Pulsed laser deposition PLD using single and dual-pulsed lasers system (SPL and DPL) was performed on targets of oyster shells Figure 1 (a, b, c). Oyster shells are natural biocomposite consisting mainly of chitin polymer dispersed in a matrix of calcium carbonate $CaCO_3$. Traces of other inorganic and organic compounds are also specific to this natural biomaterial due to phenomena and process in connection with the environmental conditions resulting into adsorption of gas components, food and enzymatic reactions during organism's lifetime.

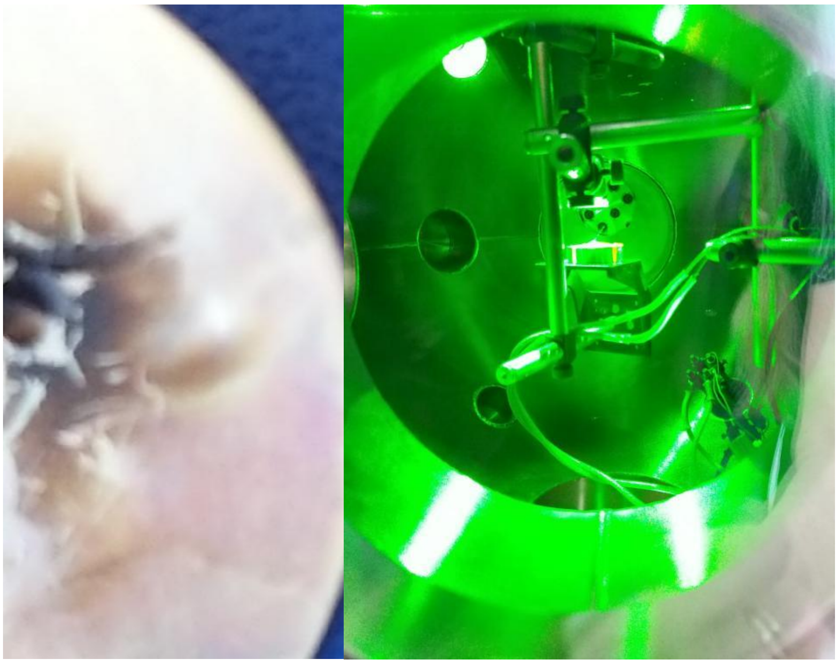

(a) (b)

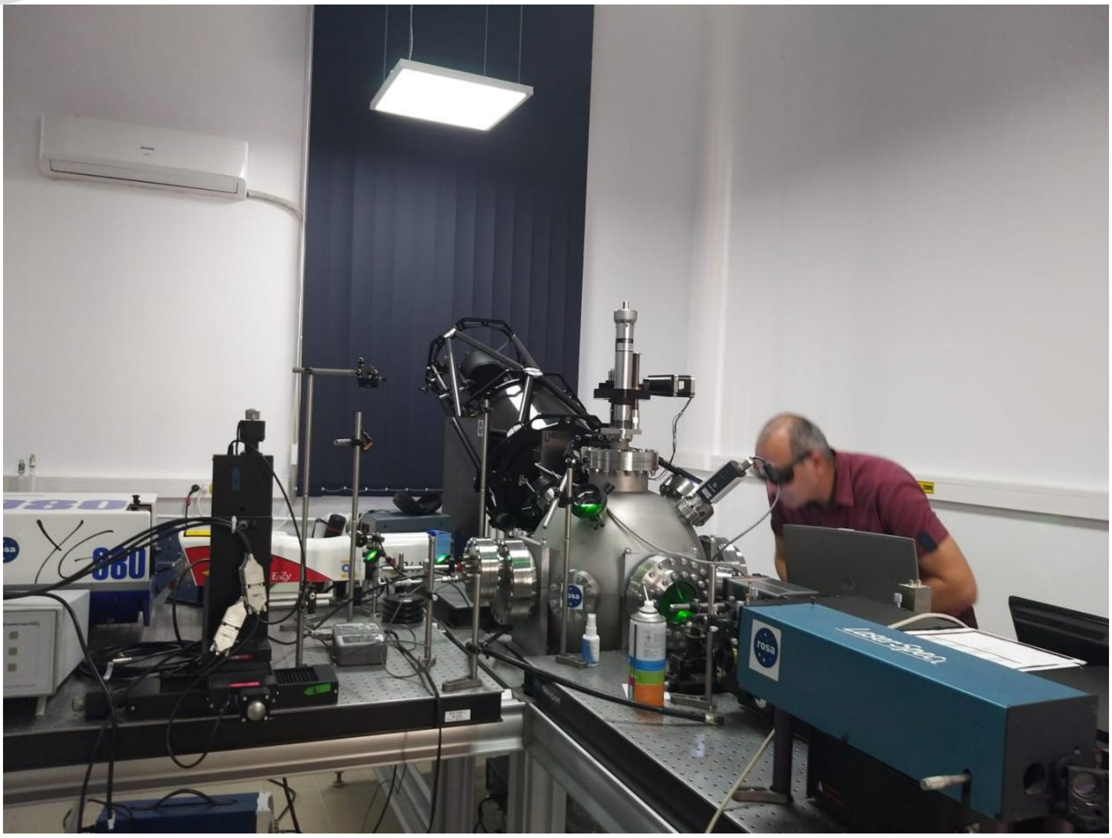

(c)

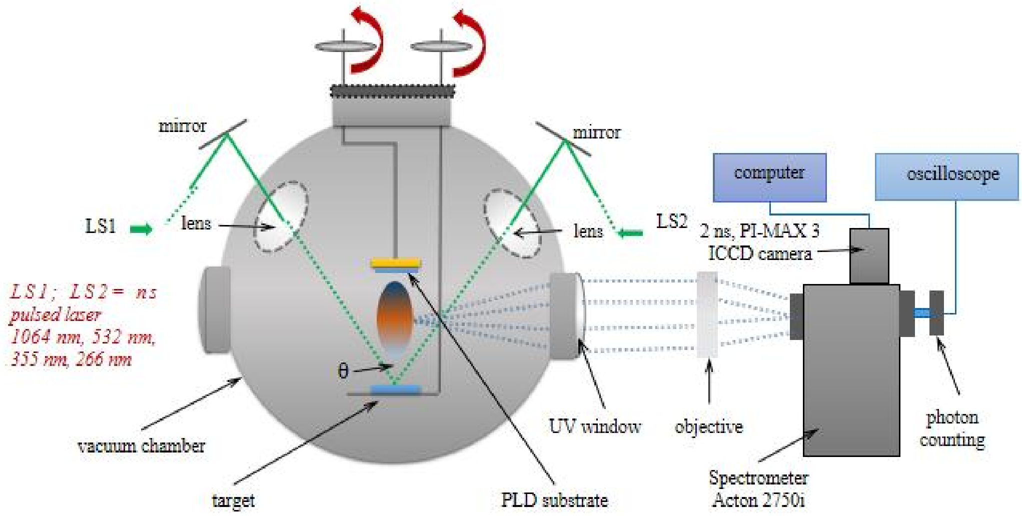
mirror
mirror
LS1
lens
lens
LS2
computer
oscilloscope
2 ns, PI-MAX 3
ICCD camera
LS1; LS2 = ns
pulsed laser
1064 nm, 532 nm,
355 nm, 266 nm
θ
vacuum chamber
target
UV window
objective
PLD substrate
photon
counting
Spectrometer
Acton 2750i

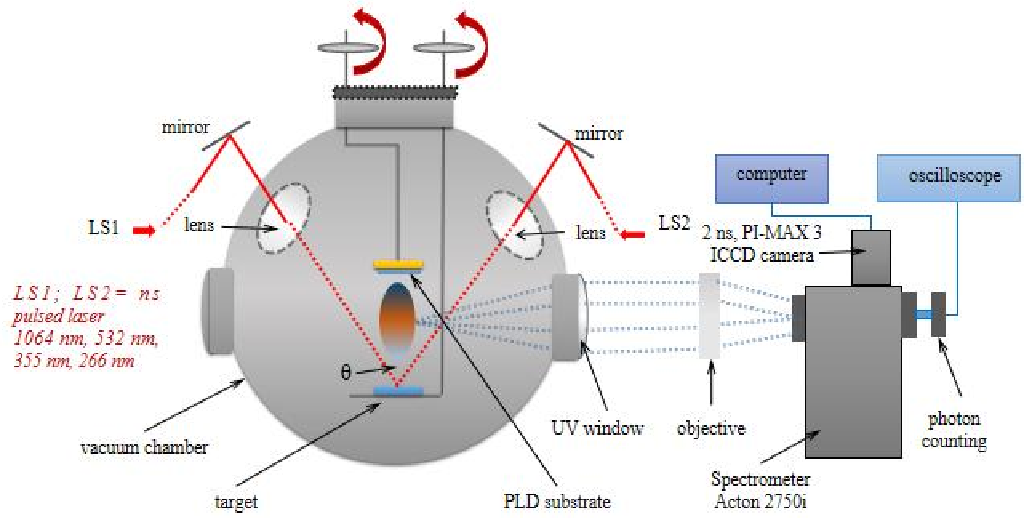

(d)

Figure 1. Images of Oyster Shell Target (a), deposition chamber during PLD performed with dual-pulsed lasers system on oyster shell target (b), installation during work (c) and schematic representation of PLD installation with dual-pulsed lasers system (d)

In the experiment, two laser systems were used in simultaneous regime and each system worked at the parameters as it follows: 30 mJ energy/sys, 10 ns each pulse width, 10 Hz pulse repetition rate, 532 nm wavelength and 300 μm spot radius of each of the laser beams of the DPL. The installation is schematically represented in Figure 1 (d).

Simulations were numerically designed using COMSOL v5.6 software to complete the information acquired during the experimental study and to optimize the system set-up.

1. Experimental and numerical results achieved in the dual-pulsed laser PLD in chitin deacetylation into chitosan (Chitin of Oyster Shell - Chitosan of Thin Film)

1.1. Experiment optimization with numerical analysis in COMSOL v5.6

Working in dual-pulsed lasers regime, a number of parameters and their combinations needs to be taken into account. Once set-up the numerical model and simulation, parameters variation make possible multiple studies in various conditions. The aim of the study is to find out the optimum way to replace a high power laser with two lower power laser systems. The results are of major interest for miniaturized devices and to and to find solutions so that the technological limits related to laser power can be exceeded.

The mathematics, theory and implementation in the soft COMSOL Multiphysics that we have already reported [1-4] have been completed with specifications and formulae to virtualy construct the two lasers’ beams interactions and their interaction with the matter. For optical constants refractive index and extinction coefficient, the Refractive index platform was used: [5]

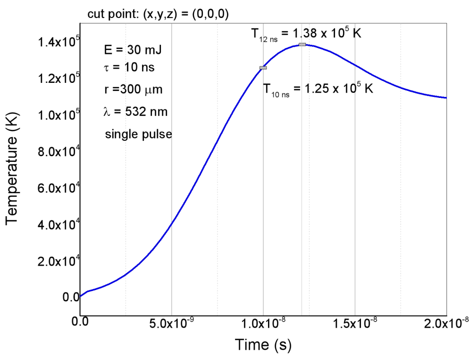

a

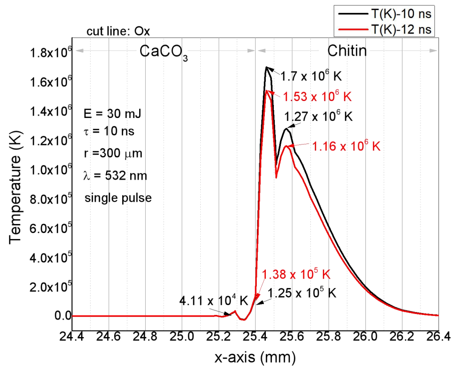

b

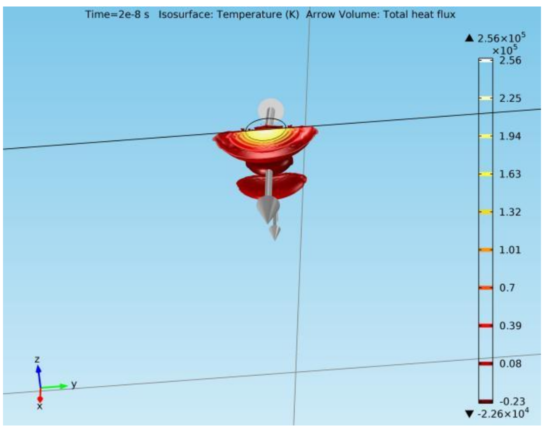

c

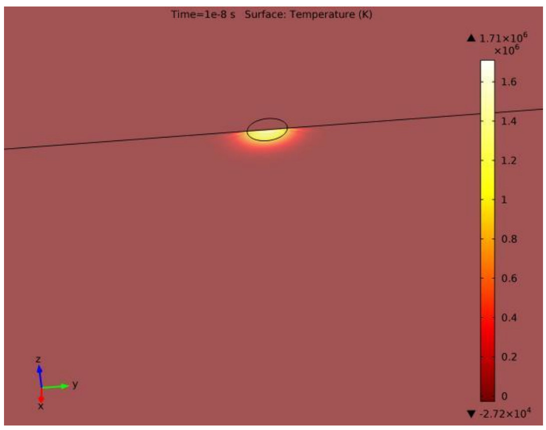

d

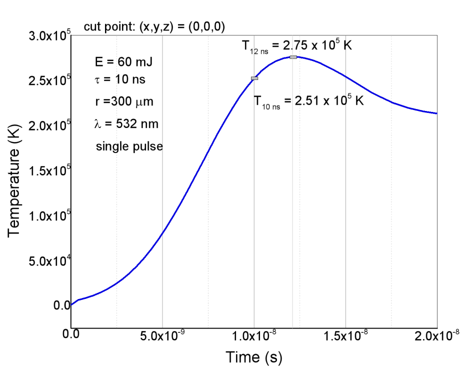
cut point: (x,y,z) = (0,0,0)
E = 60 mJ
τ = 10 ns
r =300 μm
λ = 532 nm
single pulse
T12 ns = 2.75 x 10^5 K
T10 ns = 2.51 x 10^5 K
Temperature (K)
Time (s)

e

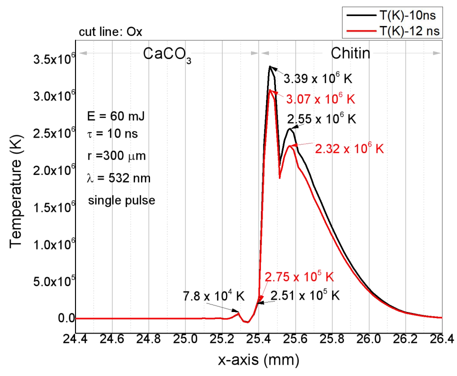
T(K)-10ns
T(K)-12 ns
cut line: Ox
CaCO3
Chitin
E = 60 mJ
τ = 10 ns
r =300 μm
λ = 532 nm
single pulse
3.39 x 10^6 K
3.07 x 10^6 K
2.55 x 10^6 K
2.32 x 10^6 K
2.75 x 10^5 K
2.51 x 10^5 K
7.8 x 10^4 K
Temperature (K)
x-axis (mm)

f

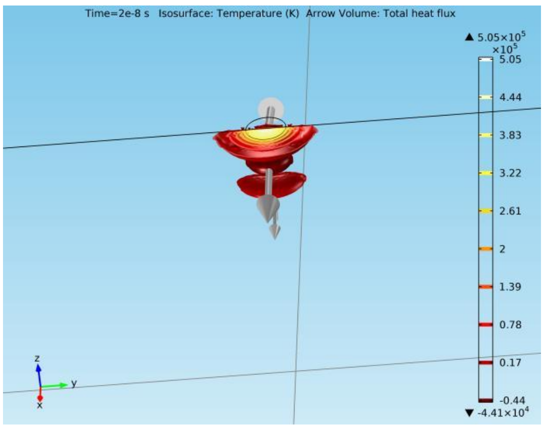
Time=2e-8 s Isosurface: Temperature (K) Arrow Volume: Total heat flux
▲ 5.05×10^5
×10^5
5.05
4.44
3.83
3.22
2.61
2
1.39
0.78
0.17
-0.44
▼ -4.41×10^4

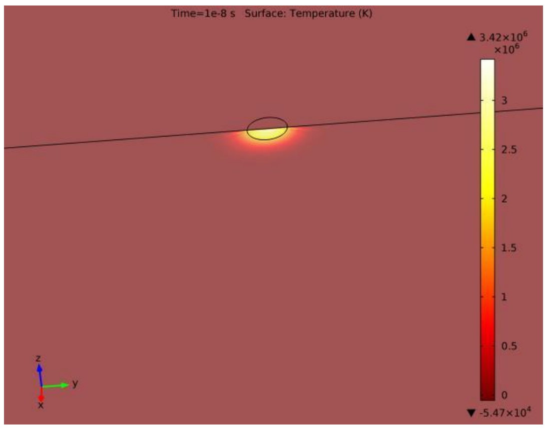
Time=1e-8 s Surface: Temperature (K)
▲ 3.42×10^6
×10^6
3
2.5
2
1.5
1
0.5
0
▼ -5.47×10^4

g

h

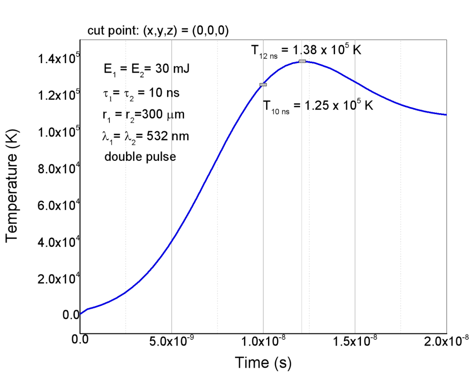
cut point: (x,y,z) = (0,0,0)
E1 = E2= 30 mJ
τ1 = τ2 = 10 ns
r1 = r2=300 μm
λ1= λ2= 532 nm
double pulse
T12 ns = 1.38 x 10^5 K
T10 ns = 1.25 x 10^5 K
Temperature (K)
Time (s)

i

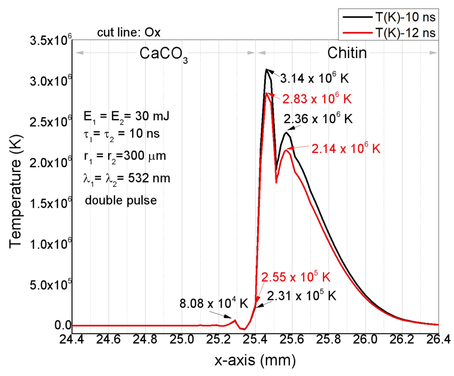
T(K)-10 ns
T(K)-12 ns
cut line: Ox
CaCO3
Chitin
E1 = E2= 30 mJ
τ1 = τ2 = 10 ns
r1 = r2=300 μm
λ1= λ2= 532 nm
double pulse
3.14 x 10^6 K
2.83 x 10^6 K
2.36 x 10^6 K
2.14 x 10^6 K
2.55 x 10^5 K
2.31 x 10^5 K
8.08 x 10^4 K
Temperature (K)
x-axis (mm)

j

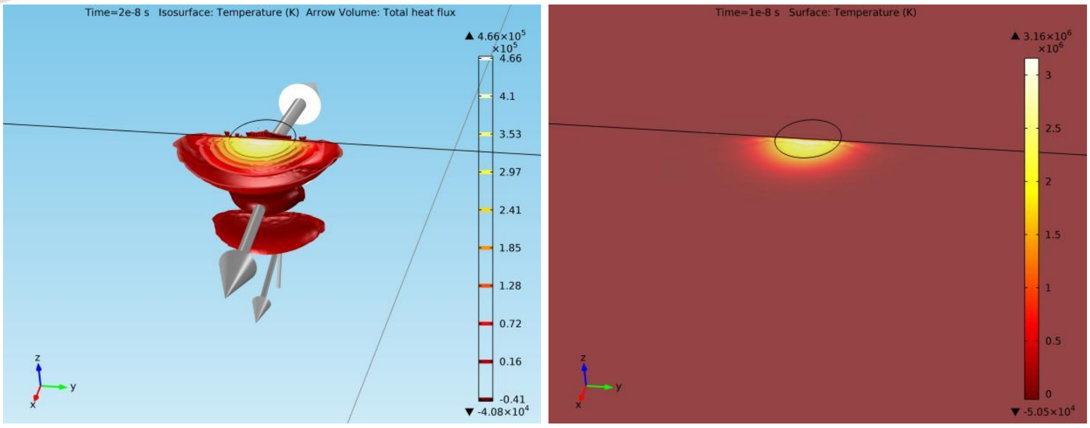

k l

Figure 2. Simulation plots with T(K) phase change diagrams for single pulsed laser systems working at different energies: 30 mJ/pulse (a, b, c, d) and 60 mJ (e, f, g, h) and dual-pulsed laser system working syncronized at 2x30mJ/pulse and 45^0 angle between the two laser beams (i, j, k, l)

Using a parametric sweep, the optimum angle between the two laser beams in the dual-pulsed lasers system was found as being 45^0. The simulation results of the dual-pulsed lasers system of 2x30 mJ/pulse (Figure 1. I, j, k, l) were compared to the results obtained when simulating laser irradiation with single pulsed laser with energies of 30 mJ/pulse (Figure 1. a, b, c, d) and 60 mJ/pulse (Figure 1. e, f, g, h) respectively. The simulations were applied to a material consisting of two components (calcium carbonate and chitin) the same as in the oyster shell used as target in the experiment. In the plots of Figure 1, the phase diagrams show that the ablation conditions are met and that similar temperatures are achieved for dual pulsed laser system 2x30 mJ/pulse as for the 60 mJ/pulse. This information is important mainly when the target laser irradiated exhibits plasma threshold at high power laser beam.

References 2.1.

[1] Georgiana Cocean, Alexandru Cocean, Cristina Postolachi, Silvia Garofalide, Georgiana Bulai, Bogdanel Silvestru Munteanu, Nicanor Cimpoesu, Iuliana Cocean and Silviu Gurlui, High-Power Laser Deposition of Chitosan Polymers: Medical and Environmental Applications. Polymers 2022, 14, 1537. https:// doi.org/10.3390/polym14081537

[2] A. Cocean, V. Pelin, M. M. Cazacua,, I. Cocean, I. Sandu, S. Gurlui, F. Iacomi, Thermal effects induced by laser ablation in non-homogeneous limestone covered by an impurity layer, Applied Surface Science 424, 324-329 (2017), http://dx.doi.org/10.1016/j.apsusc.2017.03.172

[3] A. Cocean, I. Cocean, S. Gurlui, F. Iacomi, Study of the pulsed laser deposition phenomena by means of Comsol Multiphysics, U.P.B. Sci. Bull., Series A, (Vol. 79, Iss. 2, 2017) ISSN 1223-7027

[4] A. Cocean, I. Cocean and S. Gurlui, INFLUENCE OF THE IMPURITIES TO THE COMPOSITE MATERIALS IN LASER ABLATION PHENOMENA, U.P.B. Sci. Bull., Series A, Vol. 83, Iss. 3, 2021

[5] Optical Constants of CaCO3. Available online: https://refractiveindex.info/?shelf=main&book=CaCO3&page=Ghosh-o (accessed on 12 August 2022)

1.2. **Chemical and morphological analysis of the thin film obtained in dual-pulsed laser regim compared to the single high power pulsed laser deposition**

Chemical structure of the PLD Thin Film and Thin Film2 was analyzed with Fourier Transform Infrared, a spectroscopic method for detecting functional groups with covalent bonds based on their infrared absorption properties translated into transmittance intensity versus wavenumber (cm^{-1}) spectra: Versatile FT-IR Laboratory Spectrometer MB3000, FT-IR Spectrometer Bomem MB154S spectrometer at an instrumental resolution of 4 cm^{-1} (Bomem, ABB group, Canada). Elemental composition and morphology were analyzed with Scanning Electron Microscope coupled with Energy Dispersive X-Ray (SEM-EDS) investigation with Vega Tescan LMH II, Brno, Cehia.

1.2.1. FTIR spectroscopy

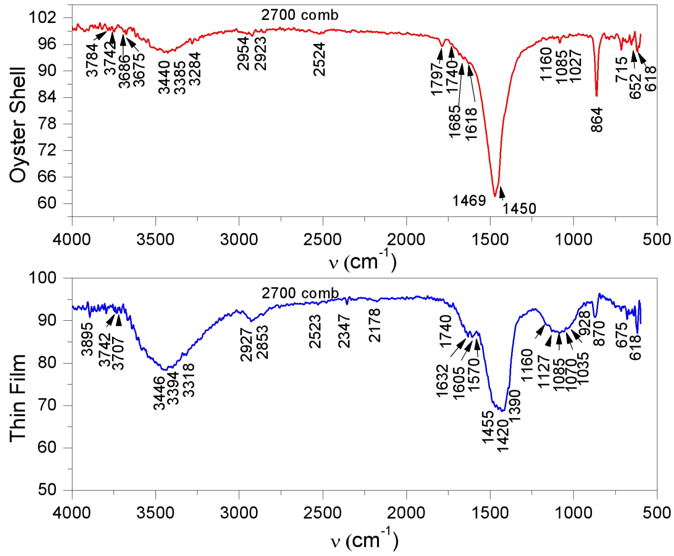

(a) [1]

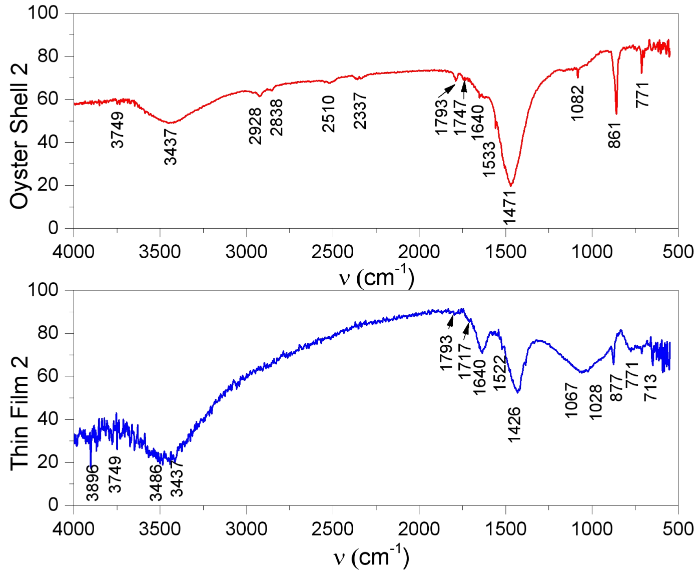

(b)

Figure 3. FTIR spectra of PLD obtained thin films with high power single pulsed laser of 150 mJ/pulse energy [] (a) and double-pulsed lasers of 2x30 mJ/pulse enery (b) compared to the targets Oyster Shell and Oyster Shell 2 (a, b).

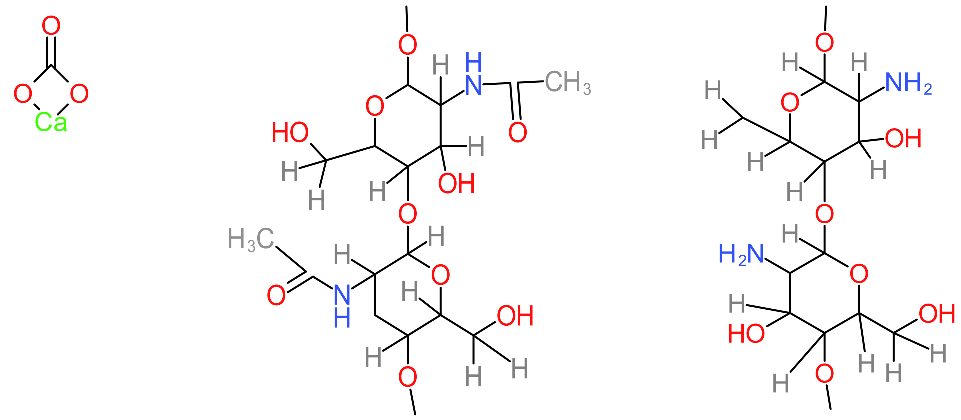

Figure 4. Oyster shell main components chemical structures calcium carbonate (a), chitin (b) and chitosan chemical structure (c)

When using **high power single pulsed laser system of 150 mJ/pulse energy**, there are clear evidences of chitin (Figure 4. b) de-acetylation process into chitosan (Figure 4.c) and calcium carbonate (Figure 4.a) decomposition into calcium oxide [1] as it follows:

Oyster Shell spectrum (Figure 3.a): the very strong band at 1469 cm^{-1}, together with bands at 864 cm^{-1} and 715 cm^{-1} for in plane and out of plane, respectively, deformations, indicate the chitin amide groups [1-7].

Thin Film spectrum (Figure 3. a): the bands at 1455 cm^{-1} and 1420 cm^{-1} evidence acetate formation together with the bands at 3446 cm^{-1}, 2523 cm^{-1}, 1632 cm^{-1}, 1570 cm^{-1} of stretching vibrations and the specific band at 928 cm^{-1} of deformation vibration of acetates [1-7]. The very intense bands at 1469 cm^{-1} in the oyster shell and 1455 cm^{-1} in the thin film are also evidence of a crystalline state and the shift denotes a change in the chemical composition that may be assigned to chitin deacetylation into chitosan and to calcium carbonate transformation into calcium oxide [1].

In the experiment with **dual-pulsed laser system of 2x30 mJ/pulse**, the changes in the chemical structure from target to deposited thin film are of similar nature as in the single pulsed laser experiment, of notice being slight shifts of the peaks and sharper and more firm shape of peaks in the fingerprint area (1717 cm^{-1} - 700 cm^{-1}). This denotes, together with the shape of the baseline, that the thin film organized in a strong crystalline structure. The Mie-scattering is very evident in the FTIR spectrum shape of Thin Film2 in Figure 3.(b) and that is assigned to crystallites of good mechanical strength because the sample was well ground in the mortar before and together with the KBr for the pellets used in the FTIR sample holder. The other aspect observed on the FTIR spectrum of the Tin Film 2 is the numerous peaks in the 4000 cm^{-1} - 3500 cm^{-1} which denote free O-H in phenols and alcohols, but also in Mg-OH, Ca-OH, Si-OH. Also, good sorption of water or aqueous solution on the Thin Film 2 is denoted by the “noisy” baseline in the 4000 - 1700 cm^{-1} range.

Oyster Shell #2 spectrum (Figure 3.a): the very strong band at 1471 cm^{-1}, together with bands at 861 cm^{-1} and 771 cm^{-1} for deformations in plane and out of plane, respectively, indicate the chitin amide groups [1-7].

Thin Film #2 spectrum (Figure 3. a): the band at 1426 cm^{-1} evidence acetate formation together with the bands at 3486 - 3437 cm^{-1}, bands in the 2500 cm^{-1} range, 1640 cm^{-1}, 1522 cm^{-1} of stretching vibrations and the specific band at 928 cm^{-1} of deformation vibration of acetates [1-7]. The very intense band at 1426 cm^{-1} in the thin film is also evidence of a crystalline state and the shift denotes a change in the chemical composition that may be assigned to chitin deacetylation into chitosan and to calcium carbonate transformation into calcium oxide [1]. The large and well defined band assigned to oxane skeletal vibrations in the range 1067 - 1028 cm^{-1} together with the enlarged peak at 771 cm^{-1} specific to CH_2 in alkanes and cycloalkanes, including herocycles shows that, in dual-pulsed lasers irradiation, the skeletal structures are well preserved and only side chain is affected by the laser irradiation, the same as in single-pulsed laser regime.

1.2.2. SEM - EDX morphological and elemental composition analyses

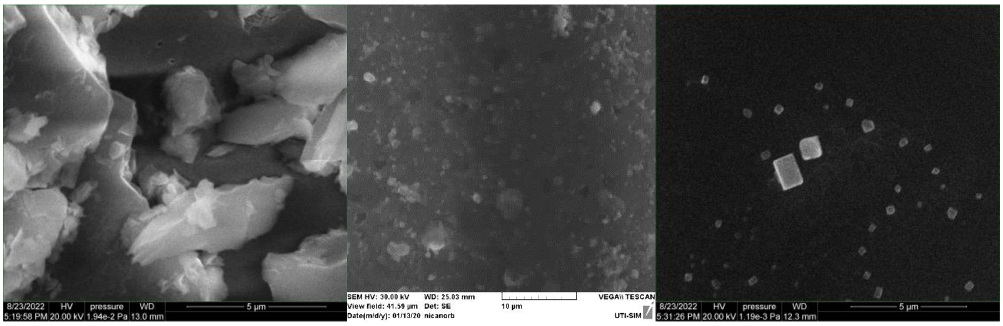

a b c

Figure 5. SEM images on oyster shell target (a), single pulsed laser deposition Thin Film (b) and dual pulsed lasers deposition Thin Film2 (c)

The images obtained with electronic microscopy (SEM) show granular structurated morphology of the Oyster Shell target (Figure 5.a) and Thin Film (Figure 5.b) while the Thin Film2 obtained in dual-pulsed laser regime, crystalline orthorombic lattice structures are clearly evidenced. The orthorombic lattice is assigned to chitosan [8] and it shows a different organization of the polymeric molecules during dual-pulsed lasers irradiation compared to single-pulsed laser irradiation.

Element	Weight %	Atomic %	Net Int.	Error %		Kratio	Z	R	A	F
C K	16.01	22.88	150.19	10.99	0.07	0.07	1.06	0.96	0.42	1
O K	61.89	66.42	544.50	10.84	0.10	0.10	1.02	0.99	0.15	1
NaK	3.86	2.88	63.66	14.85	0.01	0.01	0.93	1.01	0.16	1
CaK	18.25	7.82	1,589.98	2.39	0.16	0.16	0.87	1.06	1.03	1

a

Element	Weight %	Atomic %	Net Int.	Error %		Kratio	Z	R	A	F
C K	4.15	6.17	13.41	78.49	0.01	0.01	1.07	0.97	0.2	1
O K	63.17	70.50	980.06	8.09	0.25	0.25	1.03	0.99	0.39	1
NaK	16.26	12.63	235.55	11.24	0.03	0.03	0.93	1.01	0.21	1
MgK	3.32	2.44	72.75	13.78	0.01	0.01	0.95	1.02	0.23	1
SiK	12.78	8.12	577.44	8.06	0.05	0.05	0.93	1.03	0.45	1
CaK	0.32	0.14	17.55	28.09	0.00	0.00	0.88	1.06	0.93	1

b

Figure 6. EDS elemental composition on oyster shell target (a) and on the thin film (b)

The elemental composition shows a decrease in carbon content in the Thin Film2 which is in accordance with chitin deacetylation and calcium carbonate decomposition, in both cases, the secondary reaction products being in a gaseous state and released. Minerals like sodium and calcium remain remain adherent to the material of the thin layer in the form of impurities that can be included in the crystalline lattice or even contribute to its formation and/or to crystalline growth from crystallites.

References 2.2

[1] Georgiana Cocean, Alexandru Cocean, Cristina Postolachi, Silvia Garofalide, Georgiana Bulai, Bogdanel Silvestru Munteanu, Nicanor Cimpoesu, Iuliana Cocean and Silviu Gurlui, High-Power Laser Deposition of Chitosan Polymers: Medical and Environmental Applications. Polymers 2022, 14, 1537. https:// doi.org/10.3390/polym14081537

[2] Alexandru Cocean, Cristina Postolachi, Georgiana Cocean, Georgiana Bulai, Bogdanel Silvestru Munteanu, Nicanor Cimpoesu, Iuliana Cocean and Silviu Gurlui, The Origin and Physico-Chemical Properties of Some Unusual Earth Rock Fragments, Appl. Sci. 2022, 12, 983. https://doi.org/10.3390/app12030983

[3] A. Cocean, V. Pelin, M. M. Cazacua,, I. Cocean, I. Sandu, S. Gurlui, F. Iacomi, Thermal effects induced by laser ablation in non-homogeneous limestone covered by an impurity layer, Applied Surface Science 424, 324-329 (2017), http://dx.doi.org/10.1016/j.apsusc.2017.03.172

[4] Ernö Pretch, Philippe Bülmann, Martin Badertscher, Structure Determination Of Organic Compounds.Tables Of Spectral Data, Fourth, Revised and Enlarged Edition, Springer – Verlag Berlin Heidelberg 2009, ISBN 978 – 3 – 540 – 93810 – 1, doi 10.1007/978-3-540-93810-1

[5] Miller, F.A.; Wilkins, C.H. Infrared Spectra and Characteristic Frequencies of Inorganic Ions. Anal. Chem. 1952, 24, 1253–1294.

[6] A. Cocean, I. Cocean, N. Cimpoesu, G. Cocean, R. Cimpoesu, C. Postolachi, V. Popescu and S. Gurlui, Laser Induced Method to Produce Curcuminoid-Silanol Thin Films for Transdermal Patches Using Irradiation of Turmeric Target, Appl. Sci. 2021, 11(9), 4030. https://doi.org/10.3390/app11094030

[7] I. Cocean, A. Cocean, C. Postolachi, V. Pohoata, N. Cimpoesu, G. Bulai, F. Iacomi, S. Gurlui, Alpha keratin amino acids behvior under high fluence laser interaction. Medical applications, Applied Surface Science 488 (2019) 418–426, DOI: 10.1016/j.apsusc.2019.05.207

[8] Kenji Okuyama, Keiichi Noguchi, Takashi Miyazawa, Toshifumi Yui, and Kozo Ogawa, Molecular and Crystal Structure of Hydrated Chitosan, Macromolecules 1997 30 (19), 5849-5855, DOI: 10.1021/ma970509n

2. Conclusions

The goal of the study was 100% accomplished and the results offer valuable information on the plasma threshold during irradiation in dual-pulsed laser regime and the matter changes in its structural organization. The dual-pulsed lasers systems can be used to replace high power single-pulsed lasers systems when the latter once are not available or are not suitable for the design of the miniaturized devices. The effects of the interaction of dual-pulsed lasers systems with the matter require in-depth studies to explain phenomena related to the angle of incidence of the laser rays in relation to each other and to processes other than the thermal ones that direct the organization of matter in the plasma state induced with a dual pulsed laser. Obtaining orthographic chitosan crystals leads to the idea that, on the one hand, conditions were created to preserve some pre-existing crystallite structures in the oyster shell target and, on the other hand, conditions for crystal growth on the crystallite grains. This experiment shows that crystalline structures can be obtained by PLD method without heating the deposition substrate. The oyster shell composite structure used in the experiment provided environmental conditions as on Mars due to calcium carbonate decomposition when CO_2 is released in the deposition chamber. The initial vacuum conditions (10^{-3} Torr pressure in the deposition chamber) provided the "free of gas" environment suitable to be filled with the CO_2 and acetylene released in calcium carbonate decomposition and chitin deacetylation due to the thermal effects pulsed laser induced.

The simulation in COMSOL provided information on the optimum angle between the two incident laser beams in order to achieve maximum thermal effect in a dual-pulsed lasers system. Also, previous numerical models and simulations offered information on the expected plasma thresholds that can be achieved with different combinations of parameters and time delay in the dual-pulsed lasers irradiation of various materials used as virtual target.

The experimental results offer more information than estimated meaning that to the functional laser parameters to achieve plasma threshold required in LIBS, valuable information on the matter behavior in the conditions of dual-pulsed lasers vacuum irradiation, including, but not limited to crystals growth on crystallites preserved in conditions of plasma threshold. The study opens new perspectives of research to elucidate in-deep the phenomena noticed during experiments.

List of publications

1. Alexandru Cocean, Cristina Postolachi, Georgiana Cocean, Georgiana Bulai, Bogdanel Silvestru Munteanu, Nicanor Cimpoesu, Iuliana Cocean and Silviu Gurlui, The Origin and Physico-Chemical Properties of Some Unusual Earth Rock Fragments, Appl. Sci. 2022, 12, 983. https://doi.org/10.3390/app12030983

2. Silvia Garofalide, Cristina Postolachi, Alexandru Cocean, Georgiana Cocean, Iuliana Motrescu, Iuliana Cocean, Bogdanel Silvestru Munteanu, Marius Prelipceanu, Silviu Gurlui and Liviu Leontie, Saharan Dust Storm Aerosol Characterization of the Event (9 to 13 May 2020) over European AERONET Sites, Atmosphere 2022, 13, 493. https://doi.org/10.3390/ atmos13030493

3. Georgiana Cocean, Alexandru Cocean, Cristina Postolachi, Silvia Garofalide, Georgiana Bulai, Bogdanel Silvestru Munteanu, Nicanor Cimpoesu, Iuliana Cocean and Silviu Gurlui, High-Power Laser Deposition of Chitosan Polymers: Medical and Environmental Applications. Polymers 2022, 14, 1537. https:// doi.org/10.3390/polym14081537

4. Irimiciuc, S.; Zaharia, M.G.; Cimpoesu, R.; Bulai, G.; Gurlui, S.O.; Cimpoesu, N. On the Deposition Process of Ceramic Layer Thin Films for Low-Carbon Steel Pipe Protection. Materials 2022, 15, 4673. https:// doi.org/10.3390/ma15134673

5. Sprincean, V.; Leontie, L.; Caraman, I.; Untila, D.; Girtan, M.; Gurlui, S.; Lisnic, P.; Doroftei, C.; Carlescu, A.; Iacomi, F.; et al. Optical and Photosensitive Properties of Flexible n (p)–InSe/In2O3 Heterojunctions. Materials 2022, 15, 3140. https://doi.org/10.3390/ ma15093140

Conferences

1) Cocean, A., Postolachi, C., Cocean, G., Garofalide, S., Bulai, G., Munteanu, B. S., Cimpoesu, N., Motrescu, I., Pelin, V., Cocean, I. and Gurlui, S., High pulsed power laser inducing phase change - chemical transformations. Coupled modeling and analytical chemistry techniques. ***International Conference on Analytical and Bioanalytical Techniques, Bio Analytica 2022***; **5-7 September 20222 - speaker: Alexandru Cocean (5 september 2022)** *https://magnusconferences.com/bio-analytical-chemistry/speakers/2022* ; *https://magnusconferences.com/bio-analytical-chemistry/speaker/alexandru-coceans* *https://magnusconferences.com/bio-analytical-chemistry/uploads/pdfs/final-program-live-now.pdf*

2) Cocean, A., Garofalide, S., Pelin, V., Cocean, G., Postolachi, C., Motrescu, I. , Leontie, L., Cocean, I. and Gurlui, S., Study of the efficiency of solar cells in polluted environments: advanced analysis techniques in vivo and in the laboratory, through COMSOL type simulations, ***14th International Conference on Physics of Advanced Materials (ICPAM-14) and the 5th Autumn School on Physics of Advanced Materials (PAMS-5)***; **8-15 September 2022**, Dubrovnik, Croatia, presenting author: Silvia Garofalide.

3) Cocean, A., Postolachi, C., Cocean, G., Bulai, G., Garofalide, S., Pelin, V., Munteanu, B. S., Cimpoesu, N., Motrescu, I., Cocean, I. and Gurlui, S., Laser plasma threshold. Numerical study in COMSOL, ***International Conference ^{3}NANO 2022; Nano Science/ Technology/ Biotechnology; ROMA***, **20 - 23 September 2022**; Topic*: Theoretical modeling and computer simulations;* presenting author: Georgiana Bulai (https://www.3nano.it/home)

Project director

Prof. dr. S. Gurlui